ELECTRONIC SUPPLEMENTARY INFORMATION (ESI)

Self-assembly of Core-Polyethylene Glycol-Lipid Shell (CPLS) Nanoparticles and the Potential as Drug Delivery Vehicles

Zhiqiang Shen
Department of Mechanical Engineering, University of Connecticut, Storrs, CT 06269, USA.

David T. Loe
Department of Chemistry, University of Connecticut, Storrs, CT 06269, USA.

Joseph K. Awino
Department of Chemistry, University of Connecticut, Storrs, CT 06269, USA.

Martin Kröger
Department of Materials, Polymer Physics, ETH Zurich, CH-8093 Zurich, Switzerland

Jessica L. Rouge
Department of Chemistry, University of Connecticut, Storrs, CT 06269, USA.

Ying Li
Department of Mechanical Engineering and Institute of Materials Science, University of Connecticut, Storrs, CT 06269, USA.

E-mail: yingli@engr.uconn.edu

1. Interaction parameters

The repulsive interaction parameters a_{ij} for all kinds of bead types in the dissipative particle dynamics (DPD)simulations are given in Table S1. S, H, T, E and P represent solvent, lipid head, lipid tail, PEG and NP beads, respectively. $\mathrm{L_H}$ and $\mathrm{R_H}$ denote ligand lipid head and receptor lipid head beads, respectively. $\mathrm{L_T}$ and $\mathrm{R_T}$ represent ligand lipid tail and receptor lipid tail beads, respectively. $a_{ij} - a_{ii} = 3.27\chi_{ij}$, where χ_{ij} is the Flory-Huggins parameter. The Flory-Huggins parameters between PEG (E), lipid head (H) and lipid tails (T) beads are taken from the work done by Groot and Rabone [1], calibrated by experimental studies. Specifically, the $a_{\mathrm{SE}} = 26.3k_{\mathrm{B}}T/r_0$, which can be used to correctly predict the properties of polyethylene glycol (PEG) polymer, such as end-to-end distance and radius of gyration [2, 3], under the bond and angle potentials given in the Section 2 of main text. The nanoparticle (NP) core beads will experience a big repulsion with all other types of beads, $a_{\mathrm{Px}} = 100k_{\mathrm{B}}T/r_0$, where x represents the PEG (E), lipid head (H), lipid tails (T) and water (S) beads. The interaction parameters between the same type of beads will be taken as $25k_{\mathrm{B}}T/r_0$ [4], except for the one between NP core beads.

Table S1: Interaction parameters, a_{ij}, between beads i and j, in the DPD simulation

$a_{ij}(k_{\mathrm{B}}T/r_0)$	S	H	T	E	P	$\mathrm{L_H}$	$\mathrm{L_T}$	$\mathrm{R_H}$	$\mathrm{R_T}$
S	25.0	25.0	100.0	26.3	100.0	25.0	100.0	25.0	100.0
H	25.0	25.0	100.0	26.3	100.0	25.0	100.0	25.0	100.0
T	100.0	100.0	25.0	100.0	100.0	100.0	25.0	100.0	25.0
E	26.3	26.3	100.0	25.0	100.0	26.3	100.0	26.3	100.0
P	100.0	100.0	100.0	100.0	0	100.0	100.0	100.0	100.0
$\mathrm{L_H}$	25.0	25.0	100.0	26.3	100.0	25.0	100.0	4.0	100.0
$\mathrm{L_T}$	100.0	100.0	25.0	100.0	100.0	100.0	25.0	100.0	25.0
$\mathrm{R_H}$	25.0	25.0	100.0	26.3	100.0	4.0	100.0	25.0	100.0
$\mathrm{R_T}$	100.0	100.0	25.0	100.0	100.0	100.0	25.0	100.0	25.0

2. Self-consistent field theory

To interpret the DPD simulation results and reveal the underline physical mechanism, we employ an independent self-consistent field (SCF) theoretical approach to estimate the volume fraction profiles for each of the N (polymerization degree) monomers along a representative tethered chain separately. The SCF result allows us to calculate the radial volume fraction profile $\phi(r)$ of the spherical brush, the volume fraction profile of the terminal monomers, $\phi(r)$ and the corresponding free energy, F_{polymer}. The measured PEG profiles could be recovered using a simplest classical model of a polymer under good solvent conditions [2, 3], which is characterized by a dimensionless mixing free energy density $\nu f_m(\phi) = \tau\phi^2 + \omega\phi^3$ with $\tau = \omega = 1$, where $\nu = 0.0633\mathrm{nm}^3$ denotes the excluded volume of PEG monomer. Within

the SCF we basically aim at minimizing a single chain free energy function that is composed of elastic and interaction parts,

$$\frac{F_p}{k_{\mathrm{B}}T} = \frac{3}{2}\frac{< r_{\mathrm{ee}}^2 >}{R_0^2} + \int f_m(\phi) d^3r \tag{1}$$

where $< r_{\mathrm{ee}}^2 >= V^{-1}\int (r - d/2)^2 \phi d^3r$ is the mean squared extension of a polymer that is tethered on a sphere of diameter d, properly normalized by the occupied chain volume $V = \int \phi d^3r = N\nu$, and $R_0 = R_0(N)$ represents the equilibrium size of a PEG polymer. Here we take $R_0^2 =< R_{\mathrm{ee}}^2/e >$, using the available $R_{\mathrm{ee}}^2(N)$ values for a single PEG chain. The above free energy is minimized with respect to the volume fraction profile, subject to the constraint of conserved V and the tethering condition, $\phi(r < d/2) = 0$. A most common numerical implementation of the related optimization problem on a geometry-adapted grid have been introduced by Scheutens and Fleer [5]. We follow the implementation described in detail by Wijmans and Zhulina [6]. To this end, a single flexible polymer is grown sequentially, using a constant bond length $a = 0.33r_0$ (for PEG), starting from a spherical surface of diameter d. During random growth within the space surrounding the NP, the representative chain creates its own radial volume fraction profile to which it reacts, as the volume fraction enter the probability to choose from all possible directions, at each step of growth procedure. To be precise, it reacts by its current radial coordination r to the dimensionless exchange chemical potential $U(\phi)/k_{\mathrm{B}}T = \nu f_m'(\phi) = 2\phi + 3\phi^2$ contained in a segment weighting factor $G_1(r) = exp(-U(r)/k_{\mathrm{B}}T)$, where we recall that $\phi = \phi(r)$. The problem is thus closely related to a diffusion process in the presence of a potential and boundary, and can in principle also be formally treated using Green's functions. Accordingly, one introduces $G_n(r)$, the average statistical weight of an n-mer of which the last segment is located in layer r. $G_n(r) = G_{n-1}(r)G_1(r)$ for $n = 2, \ldots, N$, where the spatial average is taken over a sphere of radius a. We are left with a closed set of coupled equations, where the average play the role of the coefficients of a linear system of equations that can be solved in an iterative fashion using simple matrix inversions. Due to head-tail symmetry of the polymer chains, the volume fraction profile of an n-mer is subsequently obtained from the solution $G_n(r)$ via $\phi(r) = C_n G_n(r) G_{N-n+1}(r)/G_1(r)$, where the C_n's are normalization factors that follow from $\nu = \int \phi(r) d^3r$ and finally $\phi(r) = \Sigma_{n=1}^{N}\phi(r)$ as well as $\phi_N(r)$ are obtained. Because the volume fraction profiles ϕ of the unwrapped PEGylated NP are all well recorded, we can estimate the free energy difference $\Delta F_{\mathrm{polymer}} = \Delta F_p$ between wrapped and unwrapped PEGylated NP upon inserting the two measured $\phi(r)$'s separately in to Eq.1

3. Structural Analysis on CPLS NPs

To fully understand the properties of CPLS NPs, we further analyze the structure properties of these NPs, by comparing the average volume V_{polymer} and the average end-to-end distance R_{ee} for the polymer. Furthermore, we will estimate the radius of the formed CPLS NPs, as listed in the tables below. The V_{polymer} is calculated by $V_{\mathrm{polymer}} = 4\pi((R_{\mathrm{thick}} + R_{\mathrm{core}})^3 - R_{\mathrm{core}}^3)/3M$, where M represent the number of the polymer chains tethered on the NP surface. R_{thick} is

the polymer brush thickness, evaluated by $R_{\mathrm{thick}} = \int_{r_{\mathrm{core}}}^{\infty} \rho(r) r dr / \int_{r_{\mathrm{core}}}^{\infty} \rho(r) dr$ [7]. The $\rho(r)$ here is the density of the polymer. The V_{polymer} indicates the interactive chance between the individual PEG polymer. A larger value of the V_{polymer} suggests the less chance to interact with each other. While the average end-to-end distance R_{ee} of the PEG polymer reflects elasticity energy change for PEG polymers. Both of them could be used to compute the free energy change according to the SCF theory above. The radius of the CPLS NP R is calculated by $R = R_{\mathrm{core}} + R_{\mathrm{thick}} + T_{\mathrm{bilayer}}$, where R_{core} is the radius of the NP cores, T_{bilayer} is the thickness of the bilayer. The radius of the CPLS NPs will be an important parameters for the potential use in the drug delivery. And we speculate that being confined by the tethered PEG polymer, the radius of the CPLS NPs will follow a uniform size distribution.

As given in Table S2, the V_{polymer} of the polymers will change after the self-assembly according to the PEG grafting density. And the R_{ee} will increase along with the formation of the CPLS NPs. In this PEG polymerization degree $N = 10$, both of the $V_{rmpolymer}$ and the R_{ee} will not change too much. In comparison, when N increases to 40 as given in the Table S3, the end-to-end distance R_{ee} of PEG polymers will increase almost 50%. Correspondingly, the average volume for PEG polymers V_{polymer} will decrease. The significant increment of R_{ee} indicates a growth of the elastic free energy from PEG polymers. And the decreasing of V_{polymer} means that the stretched polymers will leave more space between each other, which will contribute to a reduction of the interaction free energy.

More importantly, we could find in these two tables that the radius of the CPLS NPs will almost keep a constant value as long as the PEG polymerization degrees are given (at least in the PEG density given in this paper). When $N = 10$, the variance in radius for all of the CPLS NPs is only about 2%. Even in $N = 40$ cases, the variance in radius is only 3.4%. It might indicate that even under the high PEG molecular weight, the divergence in the CPLS NPs' radius is still small. These results confirm our speculation that we are able to control the size of CPLS NPs by manipulating the PEG polymerization degree and obtain the NPs with a uniform radius distribution.

Table S2: Properties changes before and after the self-assembly process for the perfect encapsulated cases with polymerization degree $N = 10$. 'Before' in the table means that the parameters are calculated before the self-assembly process. While 'After' indicates the situation after the self-assembly process. $L = 2500$ and $L = 3000$ represent the number of the free lipids in the simulation box. σ_p is the grafting density of the PEG polymer on the NP core.

		Before			After L=2500			After L=3000	
σ_p (chains/r$_0^2$)	M	V_{polymer} (r_0^3)	R_{ee} (r_0)	V_{polymer} (r_0^3)	R_{ee} (r_0)	R (r_0)	V_{polymer} (r_0^3)	R_{ee} (r_0)	R (r_0)
0.256	80	5.111	2.345	N/A	N/A	N/A	5.495	2.553	9.625
0.384	121	3.585	2.324	3.253	2.472	9.527	3.678	2.543	9.638
0.512	161	2.877	2.382	2.722	2.508	9.622	2.812	2.543	9.654
0.64	201	2.439	2.433	2.357	2.568	9.698	2.440	2.599	9.733

Table S3: Properties changes before and after the self-assembly process for the perfect encapsulated cases with polymerization degree $N = 40$.

		Before		After L=6500			After L=7500		
σ_p (chains/r_0^2)	M M	V_{polymer} (r_0^3)	R_{ee} (r_0)	V_{polymer} (r_0^3)	R_{ee} (r_0)	R (r_0)	V_{polymer} (r_0^3)	R_{ee} (r_0)	R (r_0)
0.512	161	8.486	5.335	8.787	7.173	11.235	9.538	7.668	11.392
0.64	201	7.438	5.967	8.076	7.793	11.503	8.157	7.824	11.523
0.768	241	6.579	6.352	7.014	7.953	11.585	7.254	8.165	11.655

4. Internalization of CPLS NPs

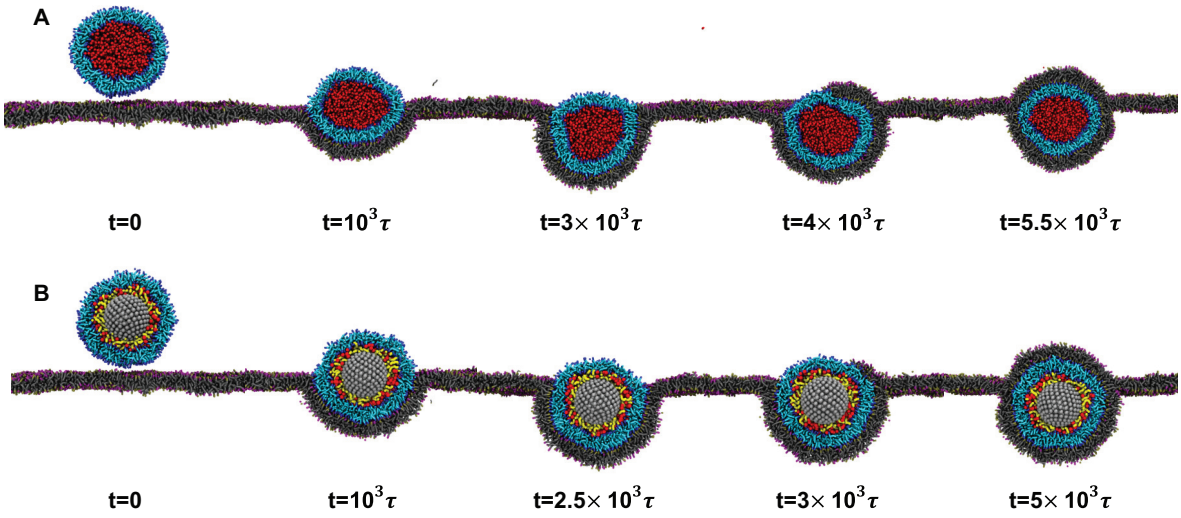

Figure S1: Lipid membrane wrapping process of (A) liposome and (B) CPLS NP, from time $t = 0$ to $t = 5500\tau$. The liposome is formed by 2500 lipid molecules. The CPLS NP is self-assembled by the PEGylated core with PEG polymerization degree $N = 10$, grafting density $\sigma_p = 0.64$ chains/r_0^2 and 2500 free lipids. The NP core is colored in sliver. The PEG polymer is colored in yellow. The lipid head and tails in the liposome and CPLS NP are colored in blue and cyan, respectively. The lipid tails in the bilayer are colored in gray. And the lipids coated with receptors in the bilayer are colored in tan, while the regular lipids heads are colored in purple. The drug molecules encapsulated within liposome and CPLS NPs are colored in red. The water beads are not shown for clarity.

The details of the membrane wrapping process of the CPLS NPs and corresponding liposome with 2500 lipids are revealed in this part. We could tell in Fig. S1 that both of the liposome and CPLS NP could be fully wrapped, conserving all the drug molecules inside after the internalization. At $t = 0$, the CPLS NP and the liposome are placed above the

lipid membrane with $3r_0$ distance respectively. Under the thermal fluctuation, both of the two NPs could easily adhere to the bilayer for the attractive interaction between the ligands and receptors. The liposome and the CPLS NP will spread on the bilayer At $t = 1000\tau$. As time evolved, at the $t = 3000\tau$, the majority of the liposome are wrapped by the bilayer, deforming to a ellipse shape. For the CPLN, it would be wrapped with the similar percentage at $t = 2500\tau$. The following protruding process will happen at $t = 4000\tau$ and $t = 3000\tau$ respectively for the liposome and the CPLS NP. At the end, both of then could be fully wrapped by the bilayer. Interestingly the CPLS NP will be fully wrapped about $t = 500\tau$ earlier than the liposome. And it might be highly related to the rigidity of the NPs [8].

5. Experimental Synthesis and characterization of CPLS NPs

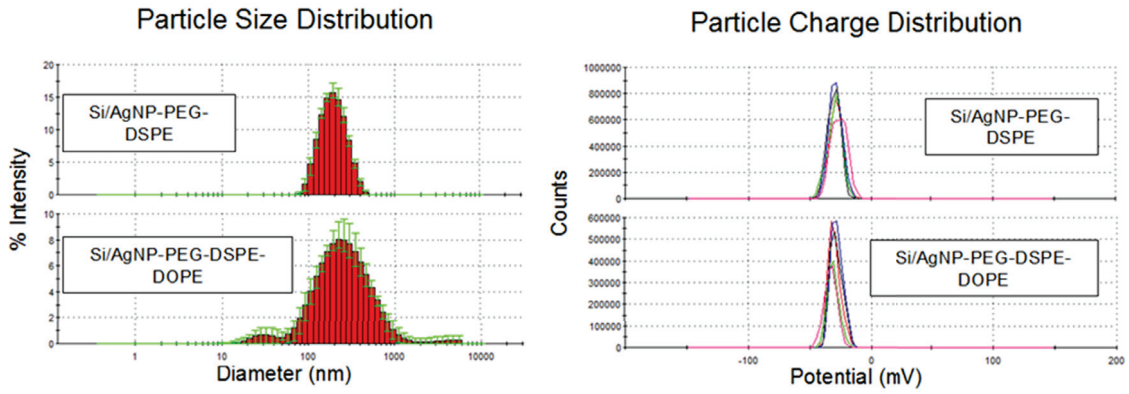

Figure S2: Representative Dynamic Light Scattering (DLS) and Zeta measurements of the CLPS NPs pre and post covalent linkage of the PEGylated lipid. The DLS of the crude synthesis (unpurified) Si/AgNP-PEG-DSPE-DOPE NPs shows a broader size distribution and some smaller materials (20-50 nm) in size which represent excess lipids which formed into micelles used in the self assembly of the lipid bilayer. This is also observed in the corresponding TEM images of the DOPE encapsulated Si/AgNP-PEG-DSPE NPs prior to size exclusion chromatography.

Table S4: Summary of particle size and charge measurements.

	AgNP-PEG-DSPE	AgNP-PEG-DSPE-DOPE	AgNP-PEG-DSPE-DOPE+Dye
Diameter (nm)	202 ± 28	399 ± 49	346 ± 19
Polydispersity	0.185 ± 0.0084	0.300 ± 0.065	0.300 ± 0.029
Surface Charge (mV)	-25.04 ± 3.65	-31.55 ± 8.23	-41.11 ± 2.36

Table S4 shows the relative size change between the PEGylated Si/Ag-PEG NP and post lipid (DOPE) encapsulation. Particles loaded with dye (CF 633) are shown for comparison in the last column. All DLS and Zeta potential measurements were run on a Malvern Zetasizer Nano ZS90. 5 measurements with 20 runs per measurement were recorded and the standard

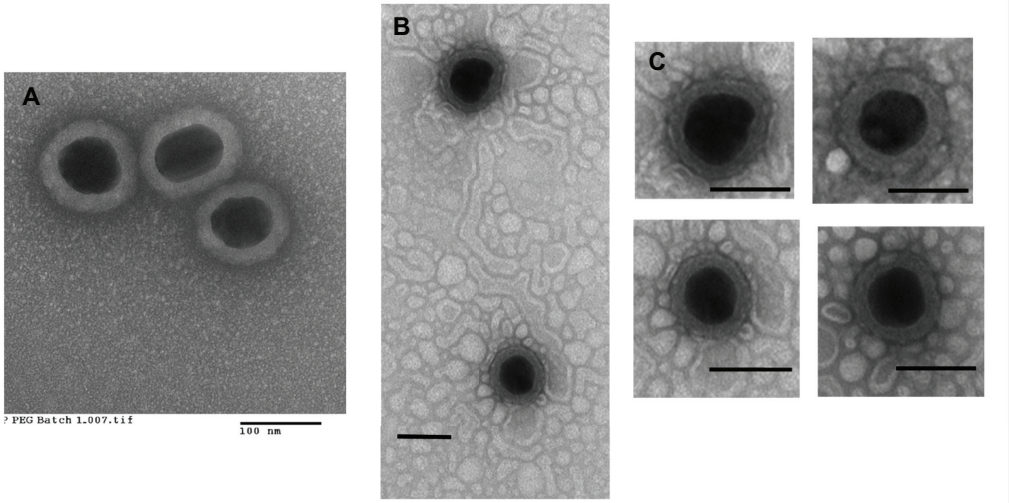

Figure S3: TEM images pre and post addition of DOPE and lipid bilayer formation. Image A shows PEGylated particles stained with uranyl acetate solution. Image B and zoomed in images C show the staining of the particles post excess DOPE addition. Edges of DOPE micelles and surface of encapsulated NPs are stained.

deviation determined per sample condition. All TEM measurements were acquired on a FEI Tecnai G2 Spirit BioTWIN Transmission Electron Microscope at the UCONN Bioscience Electron Microscopy Lab.

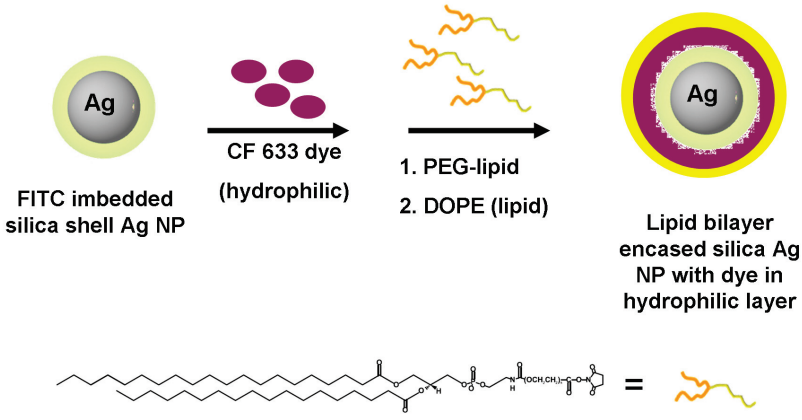

Figure S4: Schematic showing the stepwise encapsulation of a hydrophilic dye in the tethered PEG layer, beneath the outer lipid bilayer of the CPLS NP.

Dye encapsulation was performed prior to the addition of the second lipid (DOPE) during the formation of the lipid bilayer. After the Si/Ag NPs were covalently functionalized with the lipidated PEG molecule (DSPE) , they were treated with a concentrated solution of CF 633 dye (Sigma Aldrich). After adding the dye the particles were treated with DOPE in chloroform, to which dye would have been driven in the hydrophilic PEG layer of the CPLS.

Any unincorporated dye was washed away during a multistep washing and drying process. The final DOPE encapsulated particle washed of free dye was then subjected to size exclusion chromatography (SEC).

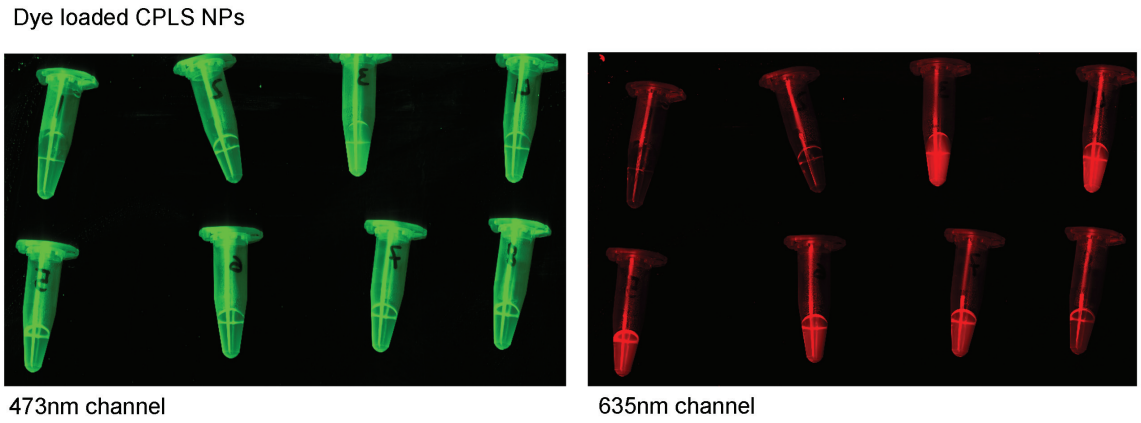

Figure S5: Green and Red channels depict laser excitation at 473 nm and 635 nm respectively. The tubes correspond to size exclusion chromatography (SEC) elution fractions (1-8) off of a G-25 sephadex column (NAP-5, GE Healthcare). The top four tubes are fractions 1-4 and the bottom are fractions 5-8. 500 μL was collected per fraction. The left image shows that the majority of the CPLS NPs elute in fraction 3. The right image shows a significant amount of dye in fraction 3, but also in fractions 4, 5, 6, and 7. This corresponds to the smaller size of the dye and that it would be expected to elute later than the larger diameter NPs. The dye found in fraction 3 is attributed to dye associated with the CPLS NPs. All fluorescent images were acquired on a GE Healthcare Typhoon FLA7000 laser gel scanner.

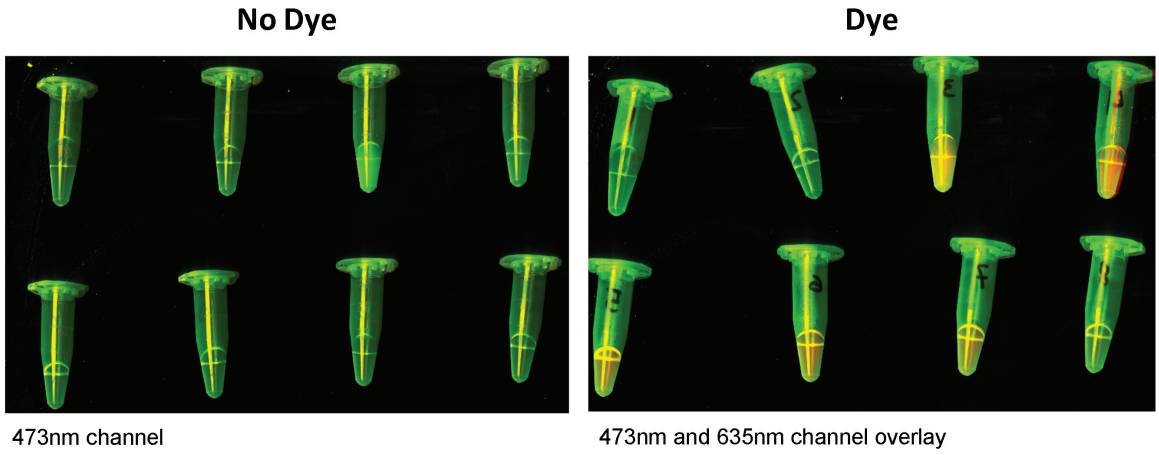

Figure S6: Green and Red channels (473 nm and 635 nm overlay) for SEC fractions of particles synthesized with and without dye. The image on the right shows that fraction 3 is the fraction in which the CPLS NPs elute. The overlain images shows the presence of both the emission of the FITC dye of the inorganic Si-Ag-NP core and the emission of the dye in fraction 3. Much of the hydrophilic small molecule dye, CF633, is encapsulated in the CPLS. Free dye is shown to elute in later fractions (4-7). All fluorescent images were acquired on a GE Healthcare Typhoon FLA7000 laser gel scanner.

Video 1.avi: Self-assembly process of a CPLS NP with polymerization degree $N = 10$ and grafting density $\sigma_p = 0.64$ chains$/r_0^2$ for PEG polymers at temperature $T = 1.0$. The number of free lipids added is 2500.

Video 2.avi: Self-assembly process of a CPLS NP with polymerization degree $N = 40$ and grafting density $\sigma_p = 0.64$ chains$/r_0^2$ for PEG polymers at temperature $T = 2.0$. The number of free lipids added is 6500.

Video 3.avi: Self-assembly process of a CPLS NP with polymerization degree $N = 40$ and grafting density $\sigma_p = 0.64$ chains$/r_0^2$ for PEG polymers at temperature $T = 1.0$. The number of free lipids added is 8000.

Video 4.avi: Self-assembly process of a CPLS NP with polymerization degree $N = 40$ and grafting density $\sigma_p = 0.512$ chains$/r_0^2$ for PEG polymers at temperature $T = 2.0$. The number of free lipids added is 6000.

Video 5.avi: Self-assembly process of a CPLS NP with polymerization degree $N = 40$ and grafting density $\sigma_p = 0.64$ chains$/r_0^2$ for PEG polymers at temperature $T = 2.0$. The number of free lipids added is 8500.

References

[1] Robert D Groot and KL Rabone. Mesoscopic simulation of cell membrane damage, morphology change and rupture by nonionic surfactants. *Biophys J*, 81(2):725–736, 2001.

[2] Ying Li, Martin Kröger, and Wing Kam Liu. Endocytosis of pegylated nanoparticles accompanied by structural and free energy changes of the grafted polyethylene glycol. *Biomaterials*, 35(30):8467–8478, 2014.

[3] Ying Li, Martin Kröger, and Wing Kams Liu. Shape effect in cellular uptake of pegylated nanoparticles: comparison between sphere, rod, cube and disk. *Nanoscale*, 7(40):16631–16646, 2015.

[4] Robert D Groot, Patrick B Warren, et al. Dissipative particle dynamics: Bridging the gap between atomistic and mesoscopic simulation. *Journal of Chemical Physics*, 107(11):4423, 1997.

[5] JMHM Scheutjens and GJ Fleer. Statistical theory of the adsorption of interacting chain molecules. 1. partition function, segment density distribution, and adsorption isotherms. *J. Phys. Chem.*, 83(12):1619–1635, 1979.

[6] CM Wijmans and Ekaterina B Zhulina. Polymer brushes at curved surfaces. *Macromolecules*, 26(26):7214–7224, 1993.

[7] Mohamed Laradji, Hong Guo, and Martin J Zuckermann. Off-lattice monte carlo simulation of polymer brushes in good solvents. *Physical Review E*, 49(4):3199, 1994.

[8] Xin Yi, Xinghua Shi, and Huajian Gao. Cellular uptake of elastic nanoparticles. *Physical Review Letters*, 107(9):098101, 2011.